Supporting Information

Tailoring Photo- and Radio-luminescence in Metal–Organic Frameworks via Coordination Groups Modulation

Chen Gong[a], Xue Han[a], Wenqian Cao[b], Guodong Qian[a], Yuanjing Cui*[b]*

[a] State Key Laboratory of Silicon and Advanced Semiconductor Materials, School of Materials Science & Engineering, Zhejiang University, Hangzhou 310027, China.

[b] Zhejiang Provincial Key Laboratory of Optoelectronic Functional Materials and Devices, ZJU-Hangzhou Global Scientific and Technological Innovation Center, School of Materials Science & Engineering, Zhejiang University, Hangzhou 311200, China. E-mail: wqcao@zju.edu.cn (W. Q. Cao), cuiyj@zju.edu.cn (Y. J. Cui)

1. Experimental Section

1.1 Reagents and Chemicals

All the reagents and chemicals were purchased from commercial sources and used directly without further purification. Tris(4-(pyridin-4-yl)phenyl)amine (TPPA, 98%) and 4,4'-(ethyne-1,2-diyl)dibenzoic acid (H_2EDBA, 98%) were obtained from Bidepharm and all metal salts were obtained from Macklin. DMF, n-propanol and ethanol were used in the synthesis processes.

1.2 Synthesis of TPPA based-MOFs

Synthesis of Zn_2(TPPA)(EDBA)$_3$.(CH_3CH_2O), ZJU-813

TPPA (4.00 mg, 0.0084 mmol), H_2EDBA (2.5 mg, 0.0094 mmol) and $Zn(NO_3)_2 \cdot 6H_2O$ (11.25 mg, 0.0378 mmol) were dissolved in N, N'-dimethyl formamide (DMF, 1 ml) and ethanol (EtOH, 1.5 ml) sealed in caped vial at 95 ˚C for 24 h. Yellow crystals were formed and collected by filtration, washed with DMF and dried in air. Yield: 60% (based on TPPA).

Synthesis of Zn_2(TPPA)(EDBA)$_3$.(NO_3), ZJU-814

TPPA (4.00 mg, 0.0084 mmol), H_2EDBA (2.5 mg, 0.0094 mmol) and $Zn(NO_3)_2 \cdot 6H_2O$ (11.25 mg, 0.0378 mmol) were dissolved in N, N'-dimethyl formamide (DMF, 1 ml) and n-propanol (NPA, 1.5 ml) sealed in caped vial at 95 ˚C for 24 h. Yellow crystals were formed and collected by filtration, washed with DMF and dried in air. Yield: 70% (based on TPPA).

Synthesis of Zn_2(TPPA)(EDBA)$_3$.(Cl), ZJU-815

TPPA (4.00 mg, 0.0084 mmol), H_2EDBA (2.5 mg, 0.0094 mmol) and $ZnCl_2$ (5.15 mg, 0.0378 mmol) were dissolved in N, N'-dimethyl formamide (DMF, 1 ml) and n-propanol (NPA, 1.5 ml) sealed in caped vial at 95 ˚C for 24 h. Yellow crystals were formed and collected by filtration, washed with DMF and dried in air. Yield: 72% (based on TPPA).

Synthesis of Zn_2(TPPA)(EDBA)$_3$.(Br), ZJU-816

TPPA (4.00 mg, 0.0084 mmol), H_2EDBA (2.5 mg, 0.0094 mmol) and Br_2Zn (8.51 mg, 0.0378 mmol) were dissolved in N, N'-dimethyl formamide (DMF, 1 ml) and n-propanol (NPA, 1.5 ml) sealed in caped vial at 95 ˚C for 24 h. Yellow crystals were formed and collected by filtration, washed with DMF and dried in air. Yield: 45% (based on TPPA).

2. Characterization and measurements

2.1 Material characterization

Powder X-ray diffraction (PXRD) patterns were recorded on an X'Pert PRO diffractometer in the range of 2θ = 5–50° at room temperature using Cu K_α radiation (λ = 1.542 Å). The X-ray photoelectron spectroscopy (XPS) spectra were collected on a Thermos Fisher Scientific K-Alpha+ spectrometer. Scanning electron microscopy (SEM) images were taken on a Hitachi S4800 field-emission scanning electron microscopy (FE-SEM). UV-vis absorption spectra were collected by a Hitachi U-4100 Spectrophotometer. The photoluminescence (PL) spectra were obtained on a Hitachi F-4600 fluorescence spectrometer at room temperature with a Xenon lamp serving as an excitation light source. Time-resolved PL spectra were recorded by an FLS920 spectrometer equipped with a 405 nm laser (Edinburgh Instrument).

2.2 Measurements of RL Spectra and Intensity

Radioluminescence (RL) spectra were measured in an experimental system consisting of an X-ray tube (Moxtek TUB00154-SA-W06, tungsten target and P_{max} = 12 W) and a fiber-coupled fluorescence spectrometer (Ocean Optics QE PRO) and a quartz mold containing the scintillator powder sample. The corresponding RL intensity can be calculated by integrating the RL spectrum collected by the spectrometer. The RL spectra of scintillator powders under different radiation doses were recorded in the same setup.

2.3 Calculation of the X-ray absorption coefficient and attenuation efficiency

The attenuation cross-section ($c(\varepsilon)$) of the scintillator was obtained from the XCOM database of the National Institute of Standards and Technology. The X-ray absorption coefficient (α) of the scintillator can be defined as follows:

$$\alpha = c(\varepsilon) \times \rho \qquad (2)$$

Where ε is the X-ray photon energy and ρ is the density of the scintillator. The X-ray attenuation efficiency (AE(d)) of the scintillator can be calculated by equation (3):

$$AE(d) = (1 - \exp(-c(\varepsilon)\rho d)) \times 100\% \qquad (3)$$

where d is the thickness of the scintillator.

3. Supplementary Tables and Figures

Table S1. Crystal data and structure refinement for ZJU-813 (CCDC 2499849).

MOF	ZJU-813
Empirical formula	$C_{118}H_{82}N_8O_{14}Zn_4$
Formula weight	2097.39
Temperature/K	170.15
Crystal system	monoclinic
Space group	$P2_1/n$
a/Å	17.6725(13)
b/Å	17.4629(12)
c/Å	22.6758(16)
α/°	90
β/°	103.141(2)
γ/°	90
Volume/Å^3	6814.8(8)
Z	2
ρ_{calc}g/cm^3	1.022
μ/mm^{-1}	0.747
F(000)	2156.0
Crystal size/mm^3	0.326 × 0.163 × 0.13
Radiation	MoKα (λ = 0.71073)
2Θ range for data collection/°	4.054 to 54.388
Index ranges	$-22 \le h \le 22$, $-22 \le k \le 22$, $-29 \le l \le 29$
Reflections collected	131145
Independent reflections	15094 [R_{int} = 0.0783, R_{sigma} = 0.0426]
Data/restraints/parameters	15094/87/756
Goodness-of-fit on F^2	1.055
Final R indexes [I>=2σ (I)]	R_1 = 0.0714, wR_2 = 0.1835
Final R indexes [all data]	R_1 = 0.1043, wR_2 = 0.2039
Largest diff. peak/hole / e Å^{-3}	0.66/-1.08

Table S2. Crystal data and structure refinement for ZJU-814 (CCDC 2499847).

MOF	ZJU-814
Empirical formula	$C_{57}H_{36}N_5O_9Zn_2$
Formula weight	1065.65
Temperature/K	200.0
Crystal system	monoclinic
Space group	$P2_1/n$
a/Å	17.7137(6)
b/Å	17.5348(6)
c/Å	22.8267(8)
α/°	90
β/°	104.503(2)
γ/°	90
Volume/Å^3	6864.2(4)
Z	4
ρ_{calc}g/cm^3	1.031
μ/mm^{-1}	1.243
F(000)	2180.0
Crystal size/mm^3	0.14 × 0.1 × 0.08
Radiation	CuKα (λ = 1.54178)
2Θ range for data collection/°	5.676 to 136.72
Index ranges	$-18 \le h \le 21$, $-19 \le k \le 21$, $-27 \le l \le 27$
Reflections collected	74792
Independent reflections	12547 [R_{int} = 0.0699, R_{sigma} = 0.0411]
Data/restraints/parameters	12547/189/811
Goodness-of-fit on F^2	1.054
Final R indexes [I>=2σ (I)]	R_1 = 0.0655, wR_2 = 0.2009
Final R indexes [all data]	R_1 = 0.0751, wR_2 = 0.2094
Largest diff. peak/hole / e Å^{-3}	0.72/-1.11

Table S3. Crystal data and structure refinement for ZJU-815 (CCDC 2499846).

MOF	ZJU-815
Empirical formula	$C_{57}H_{36}ClN_4O_6Zn_2$
Formula weight	1039.09
Temperature/K	239.0
Crystal system	monoclinic
Space group	$P2_1/n$
a/Å	17.6478(7)
b/Å	17.1561(7)
c/Å	23.3337(10)
α/°	90
β/°	106.345(2)
γ/°	90
Volume/Å^3	6779.2(5)
Z	4
ρ_{calc}g/cm^3	1.018
μ/mm^{-1}	1.563
F(000)	2124.0
Crystal size/mm^3	0.18 × 0.12 × 0.05
Radiation	CuKα (λ = 1.54178)
2Θ range for data collection/°	7.896 to 136.778
Index ranges	$-19 \leq h \leq 21$, $-17 \leq k \leq 20$, $-28 \leq l \leq 27$
Reflections collected	64025
Independent reflections	12367 [R_{int} = 0.0468, R_{sigma} = 0.0317]
Data/restraints/parameters	12367/158/736
Goodness-of-fit on F^2	1.062
Final R indexes [I>=2σ (I)]	R_1 = 0.0432, wR_2 = 0.1327
Final R indexes [all data]	R_1 = 0.0496, wR_2 = 0.1380
Largest diff. peak/hole / e Å^{-3}	0.30/-0.58

Table S4. Crystal data and structure refinement for ZJU-816 (CCDC 2499848).

MOF	ZJU-816
Empirical formula	$C_{57}H_{36}BrN_4O_6Zn_2$
Formula weight	1083.55
Temperature/K	240.0
Crystal system	monoclinic
Space group	$P2_1/n$
a/Å	17.6608(3)
b/Å	17.2165(3)
c/Å	23.5663(5)
α/°	90
β/°	107.2920(10)
γ/°	90
Volume/Å^3	6841.6(2)
Z	4
ρ_{calc}g/cm^3	1.052
μ/mm^{-1}	1.873
F(000)	2196.0
Crystal size/mm^3	0.1 × 0.08 × 0.02
Radiation	CuKα (λ = 1.54178)
2Θ range for data collection/°	5.536 to 133.938
Index ranges	$-21 \le h \le 17$, $-20 \le k \le 19$, $-28 \le l \le 27$
Reflections collected	74047
Independent reflections	12162 [R_{int} = 0.0908, R_{sigma} = 0.0545]
Data/restraints/parameters	12162/161/724
Goodness-of-fit on F^2	1.074
Final R indexes [I>=2σ (I)]	R_1 = 0.0596, wR_2 = 0.1667
Final R indexes [all data]	R_1 = 0.0921, wR_2 = 0.1870
Largest diff. peak/hole / e Å^{-3}	0.54/-0.87

Table S5. Optical Properties of the TPPA based-MOFs $k_r = \eta/\tau$, $k_{nr} = (1-\eta)/\tau$

Sample	**η (%)**	**τ (ns)**	k_r **(s^{-1})**	k_{nr} **(s^{-1})**
ZJU-813	24.32	2.00	1.22×10^8	3.78×10^8
ZJU-814	16.46	1.77	9.30×10^7	4.72×10^8
ZJU-815	17.77	1.29	1.38×10^8	6.37×10^8
ZJU-816	14.71	1.44	1.02×10^8	5.92×10^8

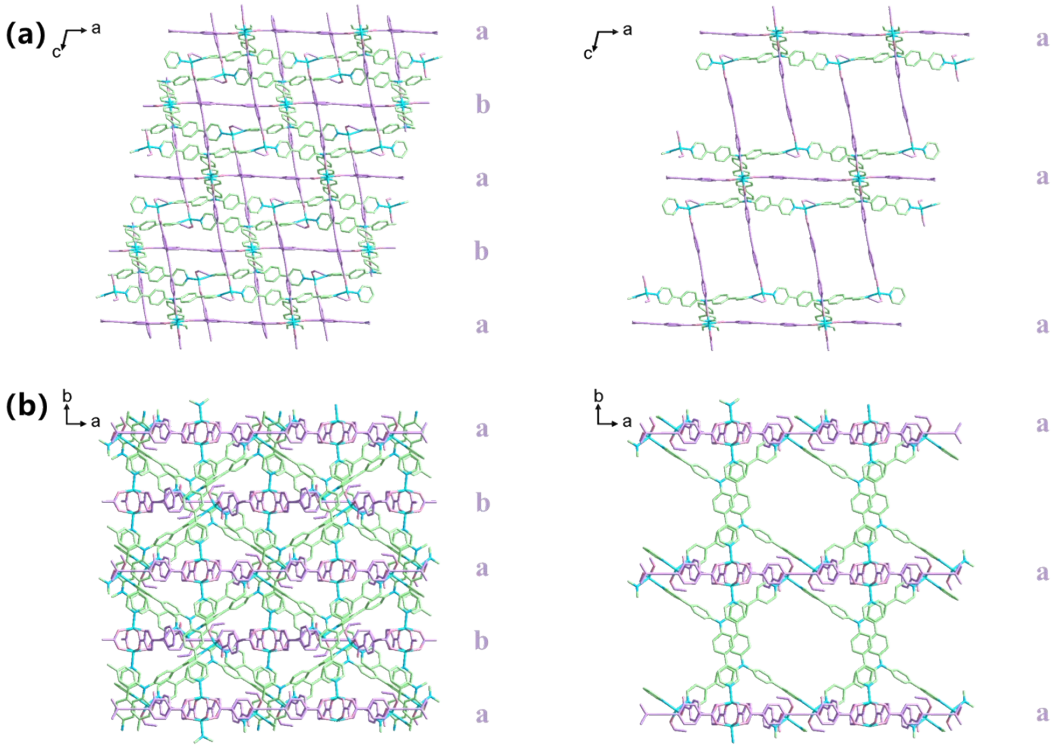

Figure S1. Crystal structure of the ZJU-813 viewed along the (a) b-axis and (b) c-axis. The monolayer network is similar to crystals aligned along the a-axis direction in that it consists solely of a-a layers or b-b layers that are connected.

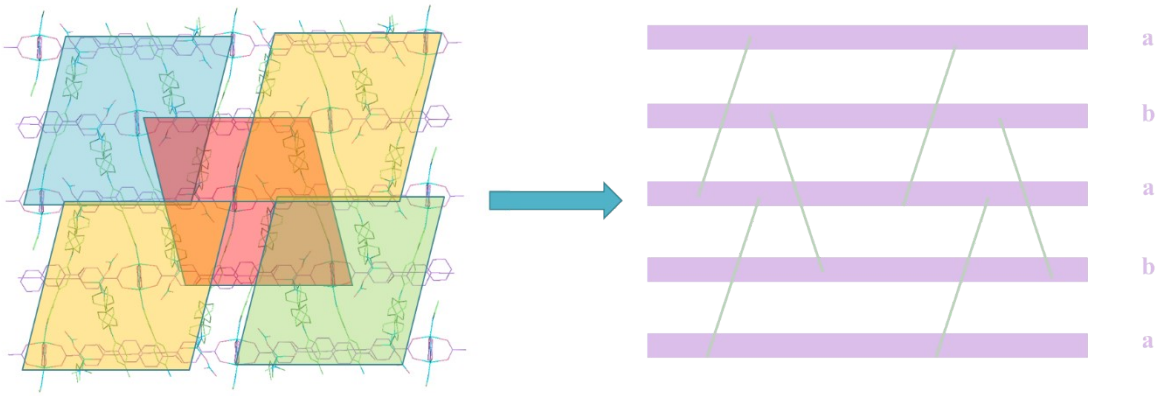

Figure S2. Crystal structure of the ZJU-814 viewed along the a-axis. Purple represents the EDBA layer formed by Zn_1 sites in a tetrahedral coordination, and green represents the TPPA ligand. Only the a-a and b-b layers are connected via TPPA; there are no a-b connections.

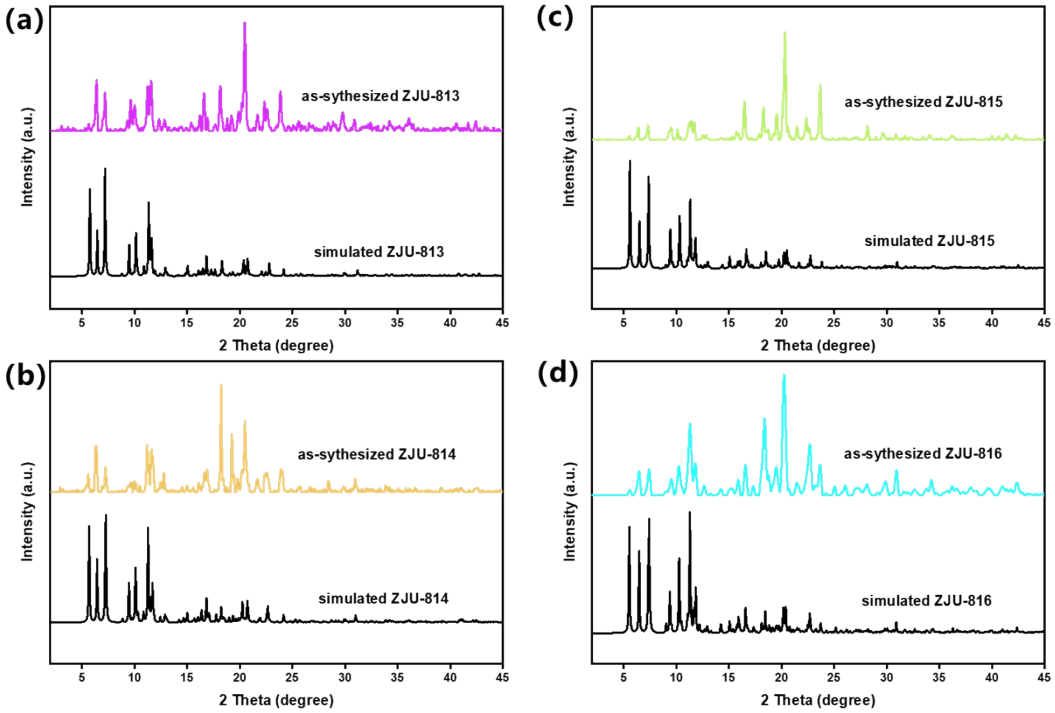

Figure S3. PXRD patterns of the four MOFs. (a) ZJU-813(b) ZJU-814 (c) ZJU-815 (d) ZJU-816. SCXRD and PXRD results provide unequivocal confirmation that these four MOFs share the same configuration.

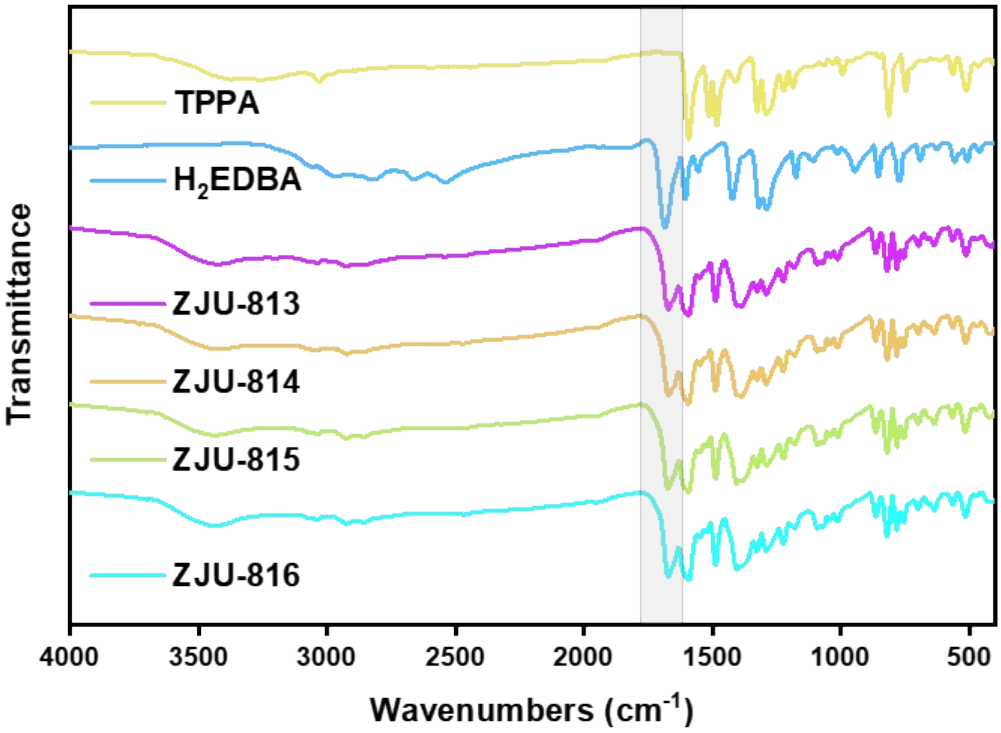

Figure S4. The FTIR spectra of TPPA and H_2EDBA powders, ZJU-813, ZJU-814, ZJU-815, ZJU-816.

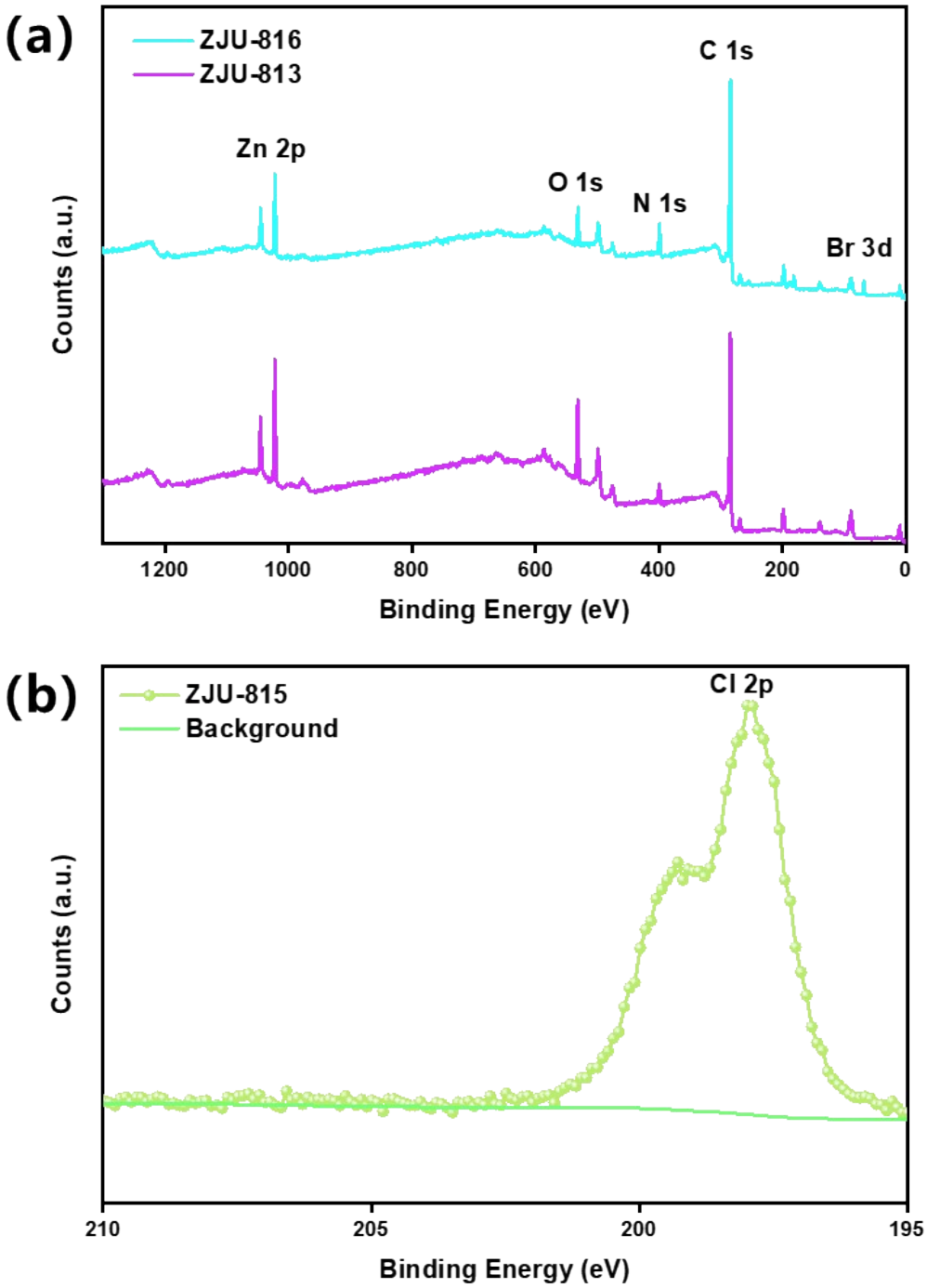

Figure S5. (a) The XPS spectra of ZJU-813 and ZJU-816, (b) XPS analysis of Cl 2p for ZJU-815, for the purpose to verify the existence of halogens.

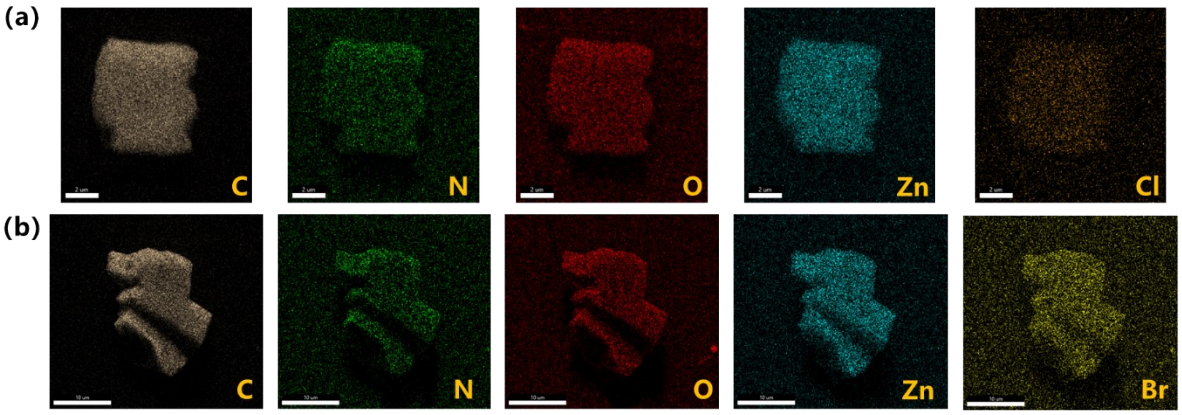

Figure S6. The EDS spectra of (a) ZJU-815 and (b) ZJU-816, for the purpose to verify the uniform distribution of halogens.

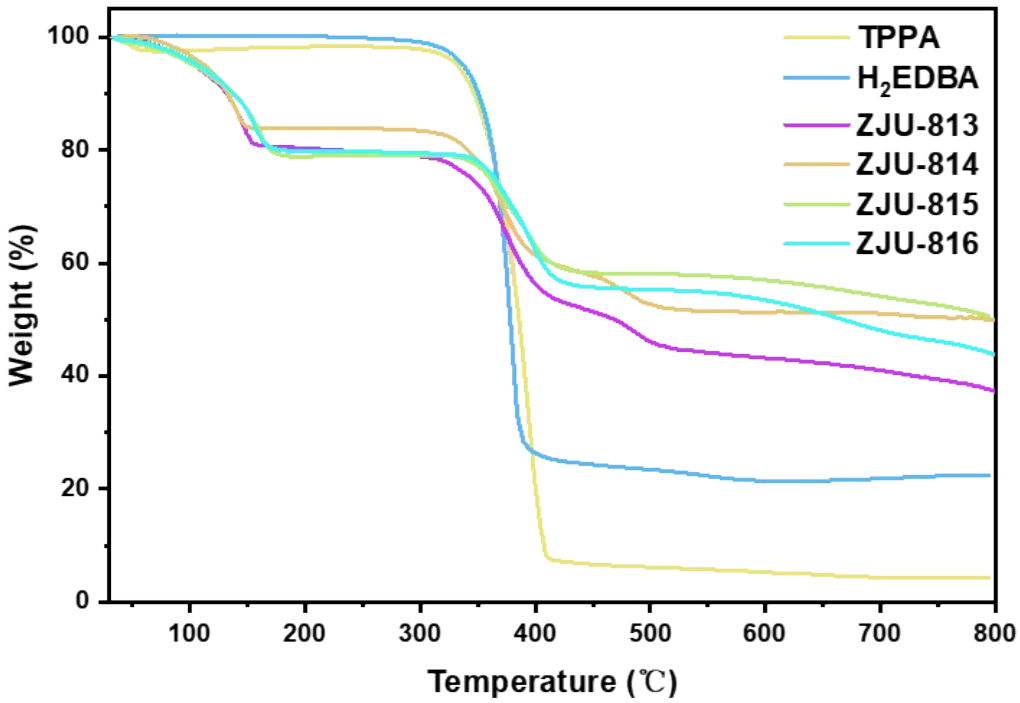

Figure S7. The TG spectra of TPPA and H_2EDBA powders, ZJU-813, ZJU-814, ZJU-815, ZJU-816.

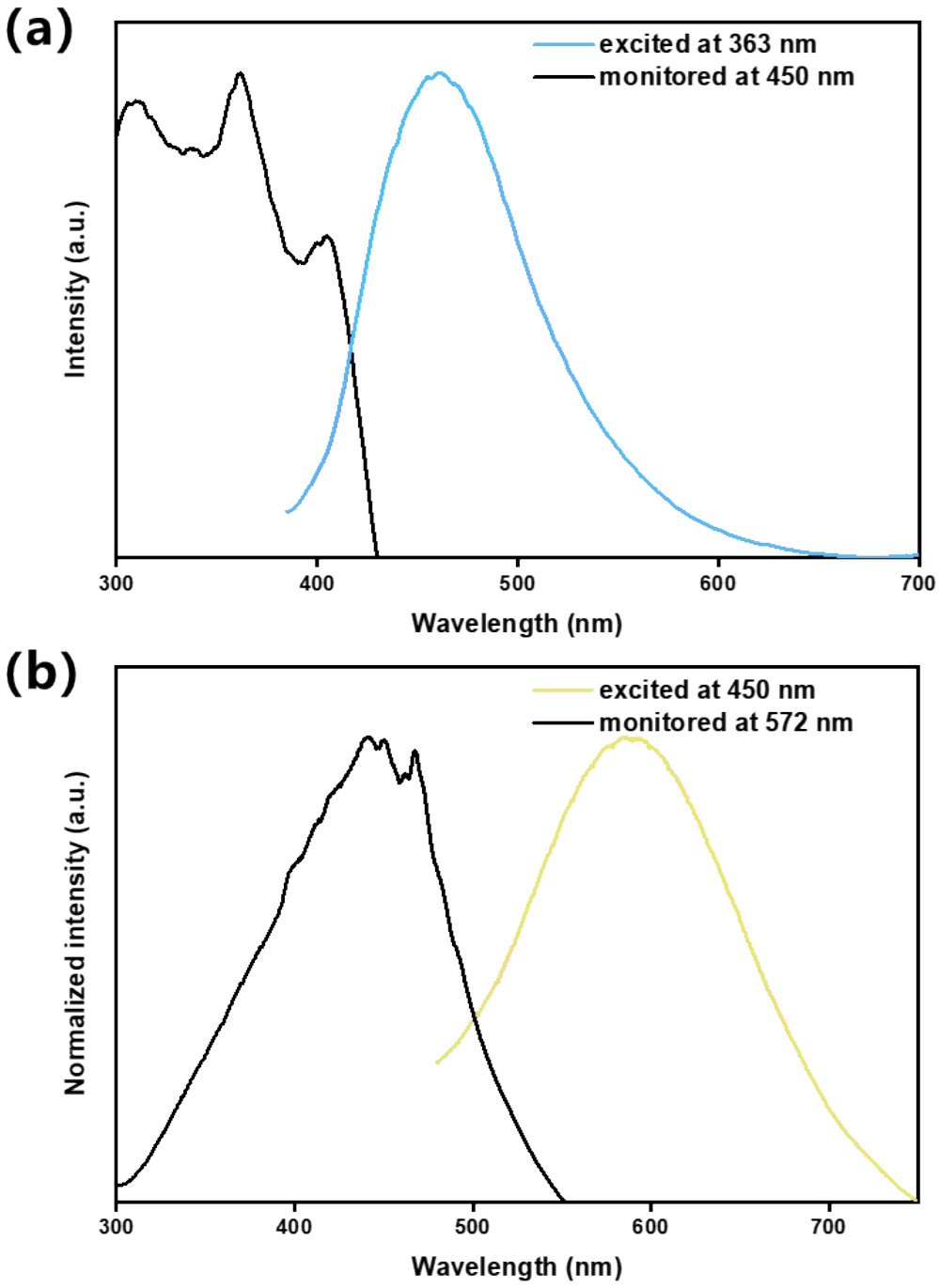

Figure S8. Excitation and emission spectra of (a) H_2EDBA and (b) TPPA ligands.

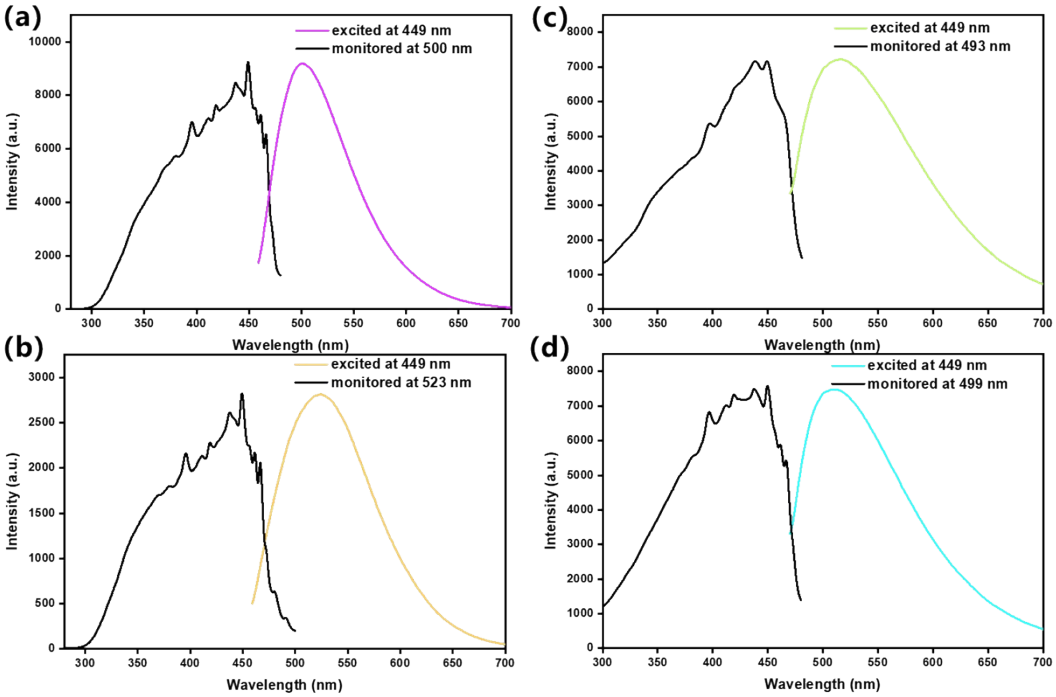

Figure S9. Excitation and emission spectra of (a) ZJU-813 (b) ZJU-814 (c) ZJU-815 (d) ZJU-816

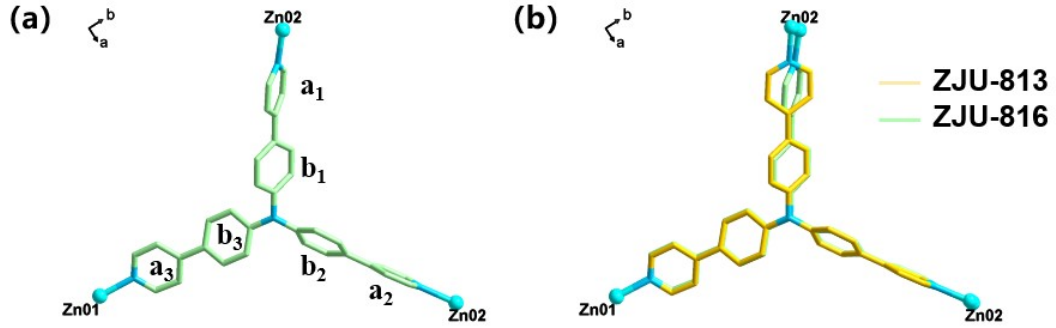

torsion angle	a_1-b_1	a_2-b_2	a_3-b_3
ZJU-813	24.587°	25.440°	27.282°
ZJU-814	24.435°	24.510°	28.790°
ZJU-815	23.862°	24.663°	30.349°
ZJU-816	28.343°	24.852°	30.102°

Figure S10. (a) The torsional angles between the adjacent pyridine rings and benzene rings in the TPPA ligand of the ZJU-813, ZJU-814, ZJU-815 and ZJU-816. (b) The structure overlay of the two crystallographocally independent molecule TPPA in ZJU-813 and ZJU-816.

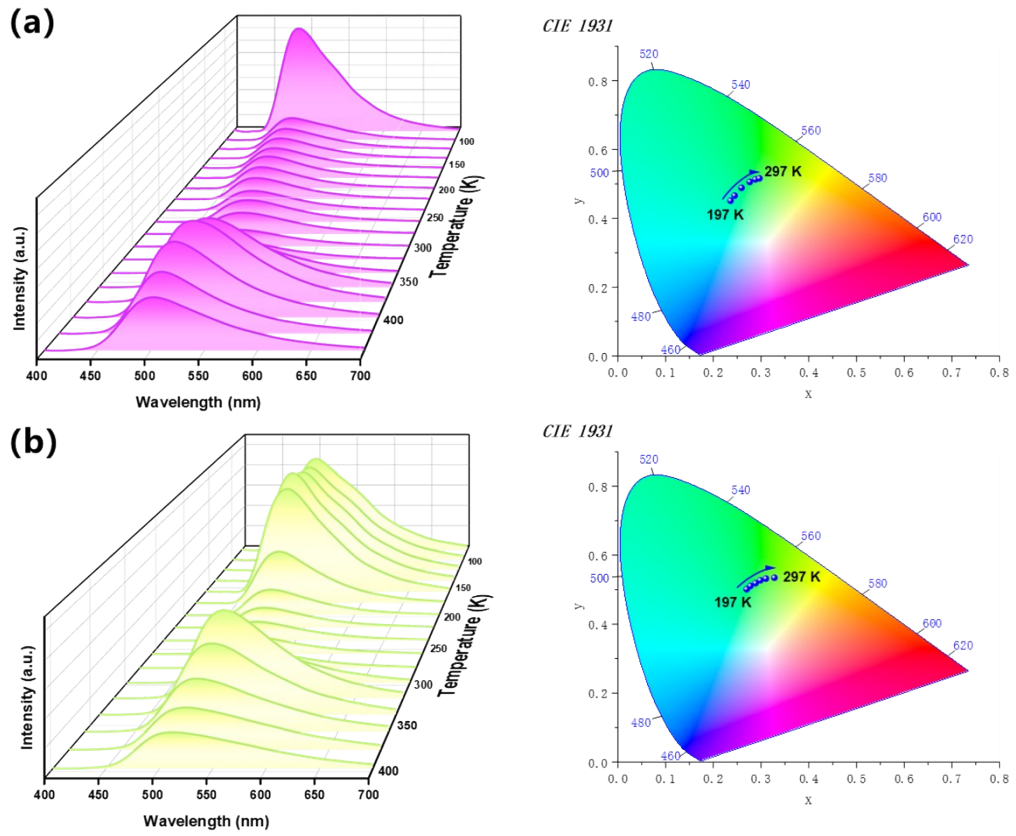

Figure S11. The fluorescence spectra after three minutes at different temperatures and the chromaticity shifts observed on the CIE coordinates correspond to the optimal emission wavelength shifts from 197K to 297K of (a) ZJU-813, (b) ZJU-815

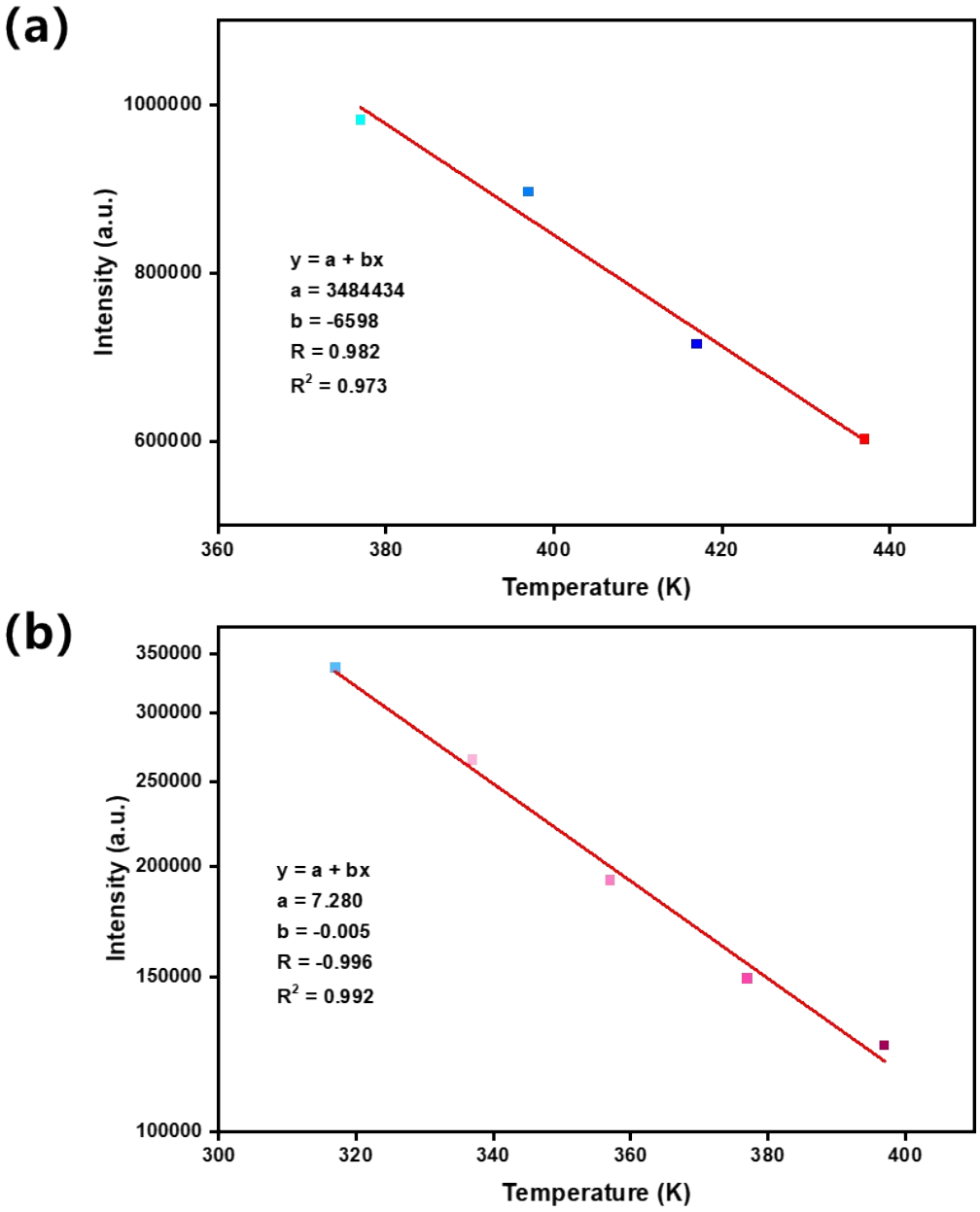

Figure S12. The (a) linear (b) exponential relationship between temperature and intensity during the high-temperature fluorescence decay phase of (a) ZJU-813 and (b) ZJU-815.

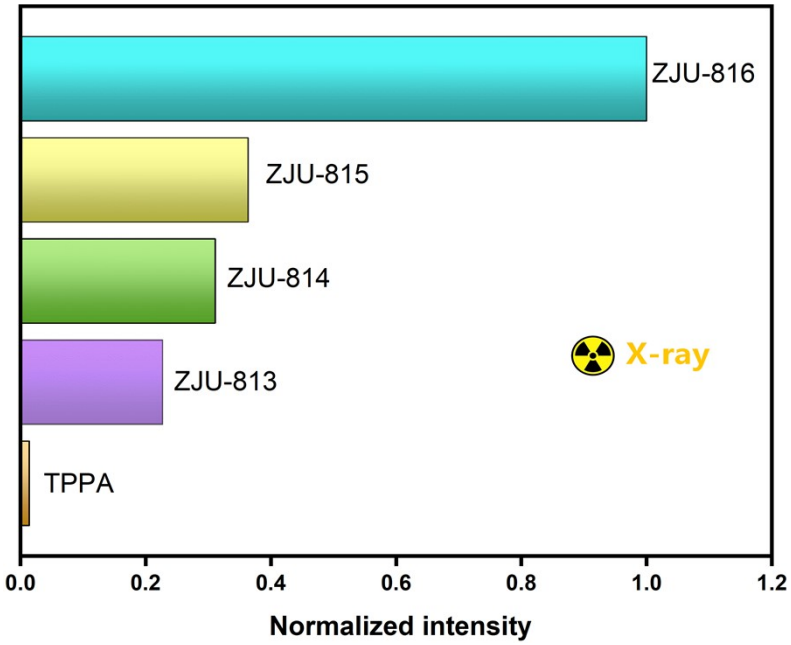

Figure S13. The normalized XEL intensity of ZJU-813, ZJU-814, ZJU-815, ZJU-816 and TPPA under the same experimental conditions

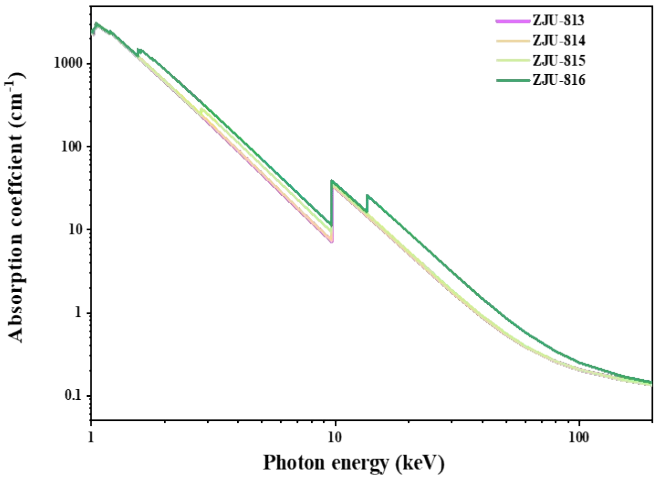

Figure S14. Absorption coefficients of ZJU-813, ZJU-814, ZJU-815 and ZJU-816.

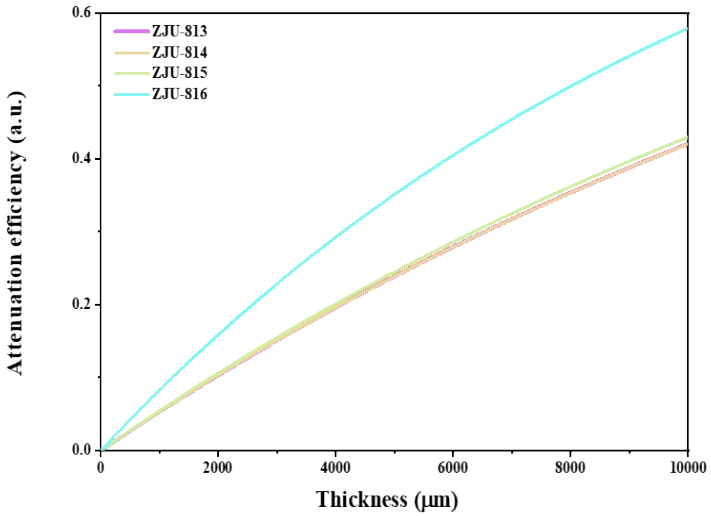

Figure S15. Attenuation efficiency of ZJU-813, ZJU-814, ZJU-815 and ZJU-816 with different thicknesses for 50 keV energy X-rays.